Journal of Solid State Chemistry 182 (2009) 215–222

Contents lists available at ScienceDirect

Journal of Solid State Chemistry

journal homepage: www.elsevier.com/locate/jssc

# Intricate 3D lanthanide–organic frameworks with mixed nodes nets

You-Gui Huang, Fei-Long Jiang, Da-Qiang Yuan, Min-Yan Wu, Qiang Gao, Wei Wei, Mao-Chun Hong *

*Key Laboratory of Optoelectronic Materials Chemistry and Physics, Fujian Institute of Research on the Structure of Matter, Chinese Academy of Sciences, Fuzhou 350002, China*

ARTICLE INFO

*Article history:*
Received 9 April 2008
Received in revised form
9 September 2008
Accepted 22 September 2008
Available online 14 October 2008

*Keywords:*
Coordination polymers
Lanthanide
Topology
Mixed nodes
Moc-related/$CdSO_4$

ABSTRACT

Three lanthanide–organic frameworks formulated as $[Yb_2(1,3\text{-pda})_3(H_2O)]_n \cdot nH_2O$ (**1**) $[La_2(2,5\text{-pydc})_3(H_2O)_2]_n$ (**2**) and $[La(2,5\text{-pydc})(2,5\text{-Hpydc})(H_2O)_2]_n \cdot nH_2O$ (**3**) ($H_2$1,3-pda = 1,3-phenylenediacetic acid, $H_2$2,5-pydc = pyridine-2,5-dicarboxylic acid) have been synthesized under hydrothermal conditions and characterized by single-crystal X-ray diffraction. Both the frameworks of compounds **1** and **2** exhibit intricate 3D architectures which can be simplified as nets with mixed nodes. Compound **1** presents a very complicated net with five types of nodes comprising intersecting (3,4)-connected and $CdSO_4$ nets. Compound **2** possesses a (4,4,6)-connected net with $(4^28^4)(4^46^2)_2(4^96^6)_2$ circuit symbol. While compound **3** is a 2D layer based upon carboxyl-bridged $La^{III}$ chains.



## 1. Introduction

Topological approach is an important tool in the design and analysis of network structures [1–10]. Wells and O'Keeffe et al. have elucidated a large number of nets of relevance to chemistry but no doubt many others await discovery [11–15]. The field of metal–organic coordination networks has witnessed tremendous success in the synthesis of interesting metal–organic frameworks (MOFs) with novel topologies [16–20]. However, in contrast to the fruitful production of (MOFs) having single node, mixed nodes networks are still scarce [21–27]. As analyzed by Ockwig, O'Keeffe, and co-workers recently, only 353 (31.3%) MOFs out of the 1127 refcodes have mixed nodes [28]. Therefore, a further study on the MOFs with mixed nodes, besides enriching the database of coordination polymers, will contribute to discovery of new topologies. Lanthanides, due to their high and variable coordination numbers and flexible coordination geometry, provide unique opportunities for discovery of interesting topologies.

As part of our ongoing search for new topologies [29], we utilize 1,3-phenylenediacetate (1,3-pda) and pyridine-2,5-dicarboxylate (2,5-pydc) as organic spacers to ligate lanthanide centers into intricate networks, and have prepared a series of lanthanide–organic frameworks with new topologies. Herein, we report the syntheses and structures of three lanthanide–organic frameworks $[Yb_2(1,3\text{-pda})_3(H_2O)]_n \cdot nH_2O$ (**1**), $[La_2(2,5\text{-pydc})_3(H_2O)_2]_n$ (**2**) and $[La(2,5\text{-pydc})(2,5\text{-Hpydc})(H_2O)_2]_n \cdot nH_2O$ (**3**).

## 2. Results and discussion

### 2.1. Synthesis

Colorless prismatic crystals of **1**, **2** and **3** were obtained by hydrothermal reactions. It should be mentioned at this point that even though the synthetic procedures of $[La_2(2,5\text{-pydc})_3(H_2O)_2]_n$ (**2**) and $[Ln_3(\mu\text{-OH})_4(2,5\text{-pydc})(2,5\text{-Hpydc})_3(H_2O)_4]_n$ are identical ($Ln$ = Sm, Eu, Gd, Dy, Yb, Y) [29], their structures are completely different. We also obtained $[Ln_2(2,5\text{-pydc})_3(H_2O)_2]_n$ ($Ln$ = Ce, Pr, Nd) in above same synthetic procedure, and these compounds are isostructural with **2**. We ascribe this phenomenon to lanthanide constriction.

### 2.2. Crystal structure of $[Yb_2(1,3\text{-pda})_3(H_2O)]_n \cdot nH_2O$ (1)

X-ray diffraction studies performed on compounds **1**–**3** reveal that all crystallize in the monoclinic system, space group $P2_1/c$. Each asymmetric unit of **1** contains two crystallographically unique $Yb^{III}$ ions, two and two half 1,3-pda ligands, a coordinated water molecule and a lattice water molecule. The local coordination geometry for the nine-coordinate Yb1 center is close to a tricapped trigonal prism by nine oxygen atoms from six 1,3-pda ligands, while Yb2 is eight coordinated by an aqua oxygen atom and seven oxygen atoms from five 1,3-pda ligands with distorted trigonal dodecahedron geometry (Fig. 1). The coordination modes of 1,3-pda in **1** are shown in Scheme 1a: four types of 1,3-pda ligands exist, 1,3-$pda^A$, 1,3-$pda^C$ and 1,3-$pda^D$ exhibit the same mode as tetra-coordinating ligands containing two chelating carboxylate groups, while 1,3-$pda^B$ as tri-coordinating ligands,

* Corresponding author. Fax: +86 591 8371 4946.
*E-mail address:* hmc@fjirsm.ac.cn (M.-C. Hong).

0022-4596/$ - see front matter © 2008 Elsevier Inc. All rights reserved.
doi:10.1016/j.jssc.2008.09.021

contains a chelating carboxylate group and a bridging carboxylate group.

The network of **1** is considerable intricate, herein we describe it step by step. The Yb centers are bridged by $\mu$-O1 and $\mu$-O3 to form chains which are further extended into a 2D layer by 1,3-pda$^{A}$ dianions (Fig. 2a). Intriguingly, a careful examination shows that the Yb1 centers are linked by 1,3-pda$^{B}$ dianions to form parallel helical chains along the crystallographic *b*-axis with a pitch of 11.267 Å (Fig. 2b). The helices ligate to Yb2 centers via O8 and share Yb1 centers with above 2D layer to form a porous 3D framework with 1D channels along the *a*-axis (Fig. 2c). In the network, each Yb1 center connects to two 1,3-pda$^{A}$ dianions and two 1,3-pda$^{B}$ dianions, each Yb2 center connects to two 1,3-pda$^{A}$ dianions and an 1,3-pda$^{B}$ dianion, consequently defining four-connecting and three-connecting node, respectively. On the other hand, each 1,3-pda$^{A}$ dianion connects to two Yb1 centers and two Yb2 centers, each 1,3-pda$^{B}$ dianion connects to two Yb1 centers and one Yb2 center, thus also defining four-connecting and three-connecting node, respectively. From the topology point of view, the Yb1 node is identical to the 1,3-pda$^{A}$ node and the Yb2 node is identical to the 1,3-pda$^{B}$ node, thus the porous 3D network can be classified as a binodal (3,4)-connected net with ($48^2$)($48^5$) Schläfli symbol (Fig. 5a). In the net, each 4-connected node connects to two adjacent ones to form a chain, which further links to four neighboring chains by 3-connected nodes, thus resulting in each 4-connected node connecting to two 4-connected nodes and two 3-connected nodes, each 3-connected node connecting to two 4-connected nodes. Finally, two adjacent 3-connected nodes connect to each other to finish the (3,4)-connected. This net is related not identical to the moc net [30], in which each 4-connected node also connects to two 4-connected nodes and two 3-connected nodes, each 3-connected node connects to two 4-connected nodes and a 3-connected node. However, in moc net, each chain formed by 4-connected nodes only links to two adjacent ones to form layers, which are further extended to 3D net by 3-connected node–3-connected node links.

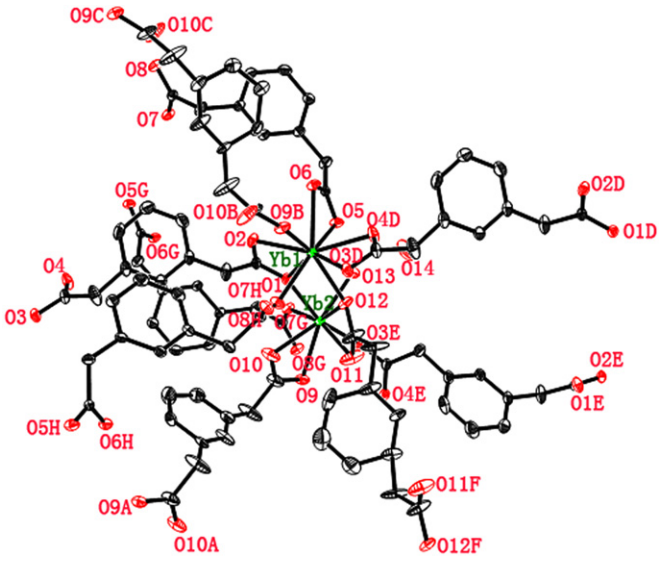


**Fig. 1.** The coordination environments of Yb1 and Yb2 atoms in **1**. Symmetry codes: A: 2−*x*, 1−*y*, −*z*; B: *x*, 1/2−*y*, 1/2+*z*; C: 2−*x*, *y*−1/2, 1/2−*z*; D: *x*−1, *y*, *z*; E: *x*−1, 1/2−*y*, *z*−1/2; F: 1−*x*, 1−*y*, −*z*; G: 2−*x*, −*y*, −*z*; H: 2−*x*, 1/2−*y*, 1/2−*z*; respectively.

On the other hand, the Yb centers are also bridged by $\mu$-O9 and $\mu$-O12 to form chains. Each chain links to four nearest neighbors via 1,3-pda$^{C}$ and 1,3-pda$^{D}$ dianions to form another 3D framework (Fig. 3). Inversion centers lie on C28 and the center of phenyl ring from 1,3-pda$^{D}$, leading to disorder of 1,3-pda$^{C}$ and 1,3-pda$^{D}$ dianions. In topology view, this net can be simplified as a $CdSO_4$ net with (6, 6) Schläfli symbol (Fig. 5b). The 1,3-pda$^{C}$ and 1,3-pda$^{D}$ dianions act as nodes and the Yb centers act as links.

The framework with (3,4)-connected net intersects with above network with $CdSO_4$ topology by sharing Yb centers to form the final intricate network of **1** (Fig. 4), which contains five types of nodes (Fig. 5c). Yb1, Yb2, 1,3-pda$^{A}$, 1,3-pda$^{B}$ define the 6-, 5-, 4-, 3-connected nodes, respectively, while 1,3-pda$^{C}$ and 1,3-pda$^{D}$ define identical 4-connected nodes different form those defined by 1,3-pda$^{A}$. As far as we know, only three one-dimensional MOFs assembled from d-block transition metal ions and 1,3-pda$^{2-}$ have been reported [31,32]. Therefore, compound 1 represents the first lanthanide–organic framework based upon 1,3-pda ligand.

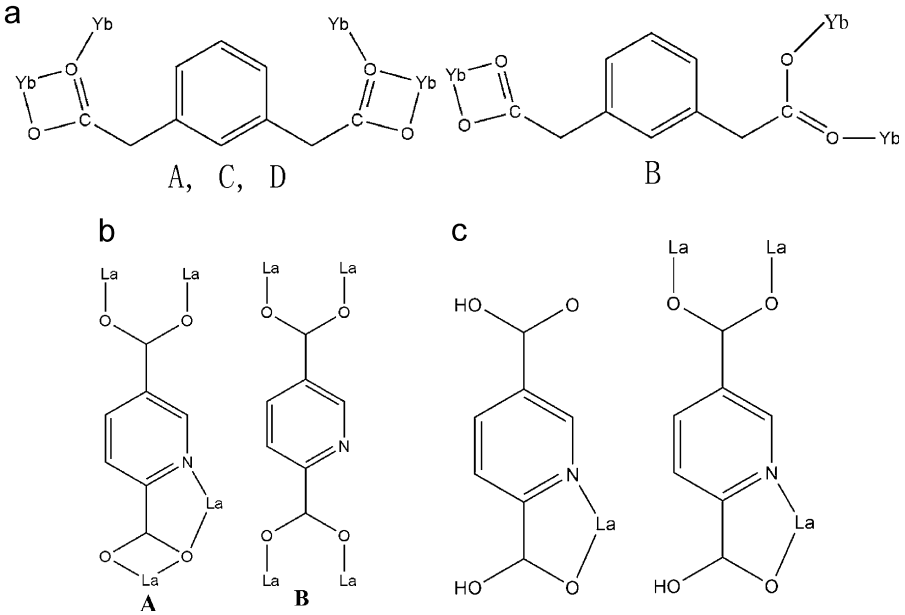


**Scheme 1.** (a) Coordination modes of 1,3-pda ligands in the structure of **1** (A = 1,3-pda$^{A}$, B = 1,3-pda$^{B}$, C = 1,3-pda$^{C}$ and D = 1,3-pda$^{D}$). (b) Coordination modes of 2,5-pydc ligands in the structure of **2** (A = 2,5-pydc$^{A}$, B = 2,5-pydc$^{B}$). (c) Coordination modes of 2,5-pydc ligands in the structure of **3**.

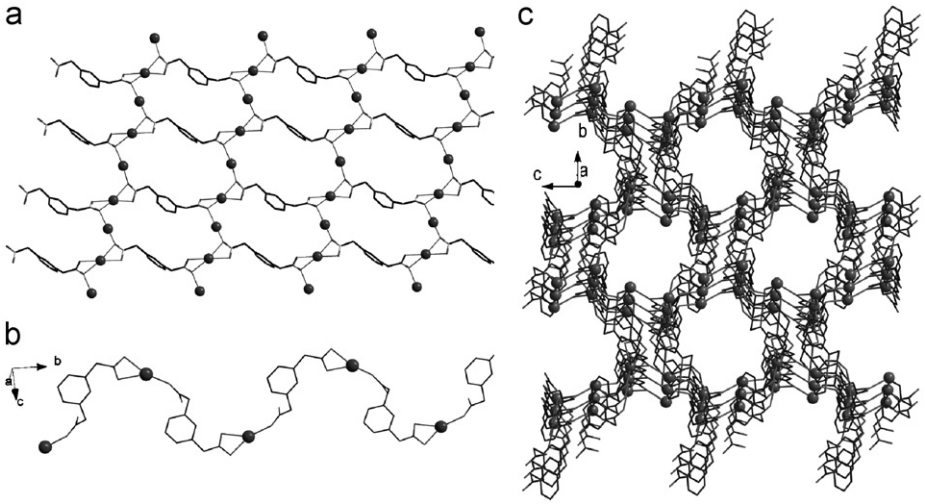


**Fig. 2.** (a) View of the 2D sheet constructed by 1,3-pda$^{A}$ dianions bridging Yb$^{III}$ centers in **1**; (b) view of the helical chain of 1,3-pda$^{B}$ dianions bridging Yb1 centers in **1**; (c) view of the three-dimensional porous moc-related network in **1**.

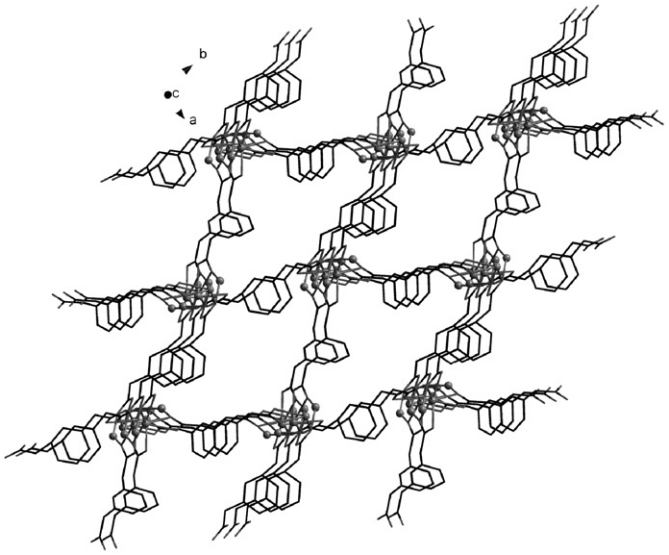


**Fig. 3.** View of the three-dimensional network with $CdSO_4$ net in **1**.

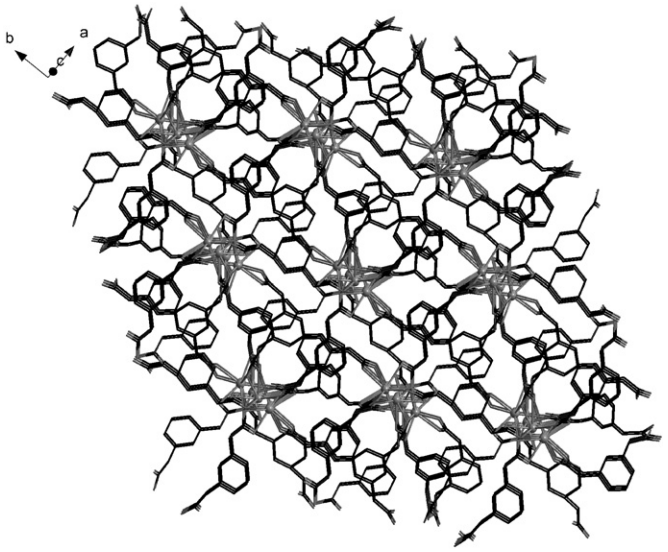


**Fig. 4.** View of the final three-dimensional network of **1**.

### 2.3. $[La_2(2,5\text{-}pydc)_3(H_2O)_2]_n$ (**2**)

The asymmetric unit of **2** contains one unique La center, one and one half 2,5-pydc dianions, and one coordinated water molecule. As shown in Fig. 6, La atom has a tricapped trigonal prism coordination with one aqua oxygen atom, one pyridyl nitrogen and seven carboxylate oxygen atoms. Two types of 2,5-pydc ligands exist in **2**, both act as tetra-coordinating ligands, 2,5-pydc$^{A}$ contains one bridging carboxylate group and one chelating carboxylate group, whereas 2,5-pydc$^{B}$ contains two bridging carboxylate groups (Scheme 1b). One inversion center lies on the center of pyridyl ring of 2,5-pydc$^{B}$ leading to the disorder of its pyridyl nitrogen.

Each La core in **2** is double bridged to two adjacent neighbors by $\mu$-O9 and O5–C7–O6 to form chains which are further extended into 2D layer through 2,5-pydc$^{A}$ dianions in the bc-plane (Fig. 7a). On the other hand, La cores are bridged by 2,5-pydc$^{B}$ dianions to form order tapes along the *a*-axis (Fig. 7b). The tapes intersect with above layer resulting in a three dimensional framework (Fig. 7c).

In the network of **2**, each La core connects to four 2,5-pydc$^{A}$ dianions and two 2,5-pydc$^{B}$ dianions, thus defining a 6-connected node; while each 2,5-pydc$^{A}$ dianion and 2,5-pydc$^{B}$ dianion connects to four La cores thus both defining 4-conncetd nodes. However, the two 4-conncetd nodes are not identical, leading to three types of nodes existing in the net. In topology view, the net can be classified as (4,4,6)-connected net with $(4^28^4)(4^46^2)_2(4^96^6)_2$ circuit symbol (Fig. 8). The circuit symbols for 2,5-pydc$^{A}$, 2,5-pydc$^{B}$ and La nodes are $(4^46^2)$, $(4^28^4)$ and $(4^96^6)$, respectively.

### 2.4. $[La(2,5\text{-}pydc)(2,5\text{-}Hpydc)(H_2O)_2]_n \cdot nH_2O$ (**3**)

The asymmetric unit of **3** contains one unique La$^{III}$ ion, one 2,5-pydc dianion, one 2,5-Hpydc anion, two coordinated and one lattice water molecules. La$^{III}$ ion is nine coordinated by two pyridyl nitrogen atoms, five carboxylate oxygen atoms and

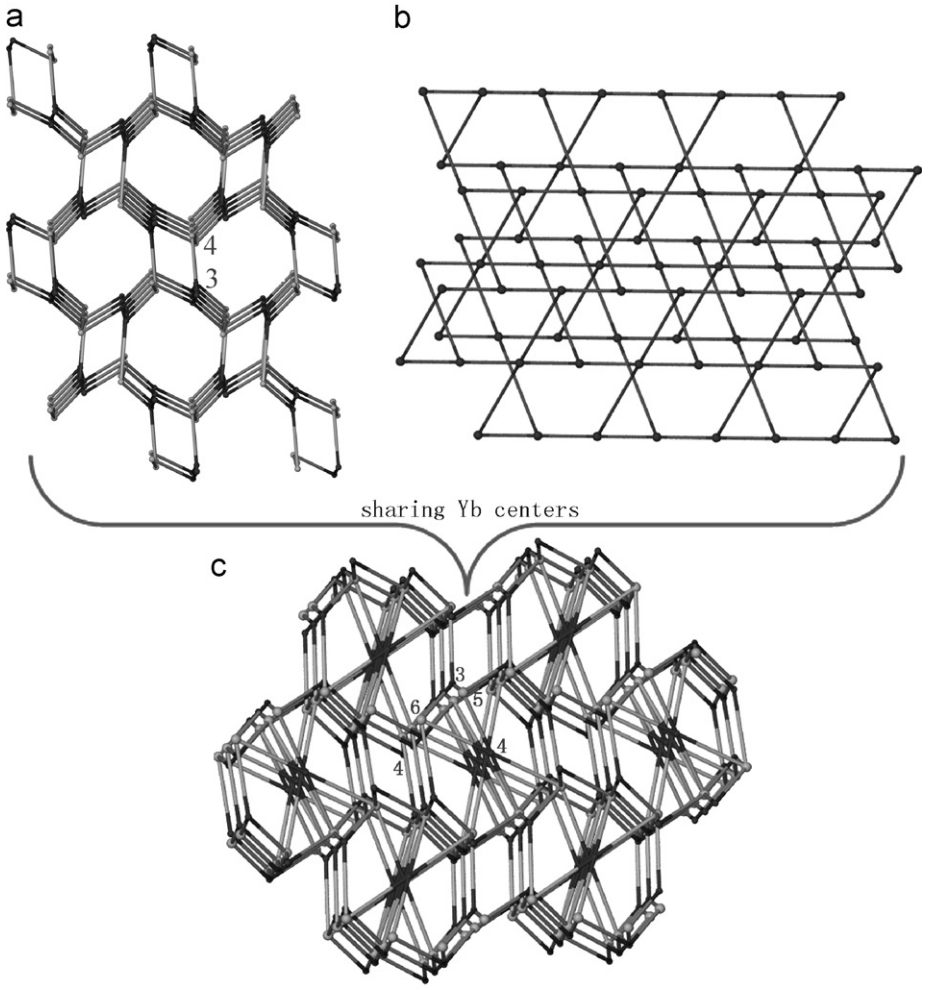


**Fig. 5.** (a) Topology view of the moc-related net in **1**. (b) Topological view of the $CdSO_4$ net in **1**. (c) Topological view of the final network of **1** with five kinds of nodes.

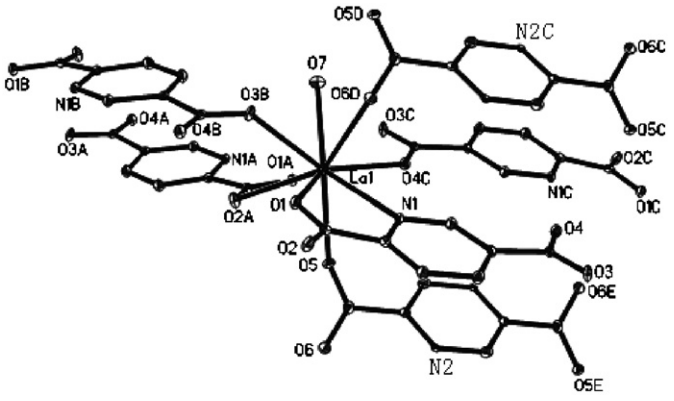


**Fig. 6.** The coordination environments of La atoms in **2**. Symmetry codes: A: *x*, 1/2−*y*, *z*−1/2; B: 1−*x*, *y*−1/2, 3/2−*z*; C: 1−*x*, 1−*y*, 1−*z*; D: *x*−1, *y*, *z*; E: 2−*x*, 1−*y*, 1−*z*; respectively.

two aqua oxygen atoms with a tricapped trigonal prism geometry (Fig. 9). The 2,5-Hpydc anion chelates to one $La^{III}$ ion using the pyridine nitrogen and one of the 2-carboxylate oxygen atoms. While the 2,5-pydc dianion acts as $\mu_3$-bridge in which the pyridine nitrogen and one of the 2-carboxylate oxygen atoms chelating a $La^{III}$ ion and the 2-carboxylate group adopts $\mu_2$-$\eta^1$:$\eta^1$-bridging mode (Scheme 1c).

$La^{III}$ ions are firstly bridged by $\mu$-O6 and 5-carboxylate group (O7–C14–O8) from 2,5-pydc dianion to form a chain (Fig. 10a). There are two different La–La distances (La⋯La = 4.398 Å, La⋯La = 5.518 Å) within the chain corresponding to two different kinds of links. Then, the chains are bridged together through the pyridine moieties of the 2,5-pydc dianions to generate a layer (Fig. 10b). The 2,5-Hpydc anions and coordinated water molecules only ligate to $La^{III}$ centers to furnish the tricapped trigonal prism geometry (Fig. 10c). The layers stack along the *b*-axis with lattice water molecules locating between them.

### 2.5. Magnetic properties

Temperature-dependent magnetic susceptibility measurement for **1** was performed on the crystalline sample in the temperature range 2–300 K under 1 K Oe external field. Fig. 11 shows the plot of $\chi_m T$ vs $T$ per $Yb_2^{III}$ unit of 1. The $\chi_m T$ value of 6.40 $cm^3\,K\,mol^{-1}$ at room temperature is slightly higher to the theoretical value of 5.07 $cm^3\,K\,mol^{-1}$. The $\chi_m T$ values decreases to a value of 2.27 $cm^3\,K\,mol^{-1}$ at 2 K. It is well known that the $4f^n$ configuration of $Ln^{III}$ ion is split into $^{2S+1}L_J$ states by the interelectronic repulsion and the spin–orbit coupling. Further splitting into stark components is caused by the crystal-field perturbation [33,34]. At room temperature, all the Stark levels arising from the degenerate $^2F_{7/2}$ ground states of $Yb^{III}$ ion are populated, but as temperature

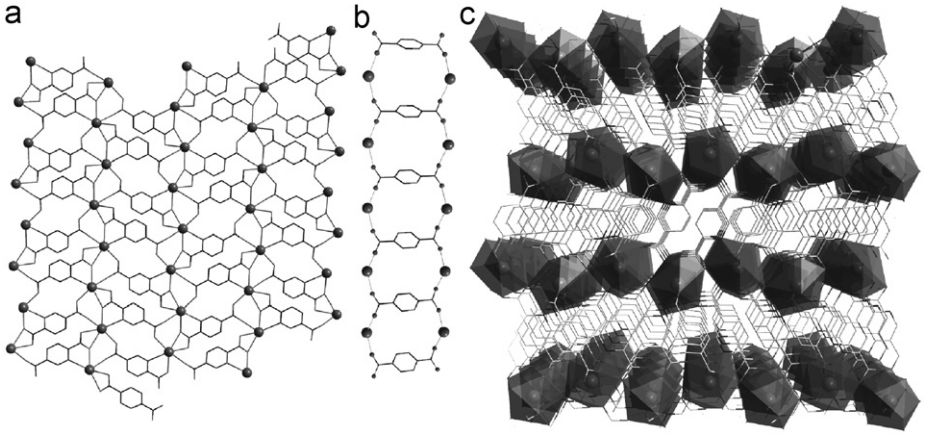


**Fig. 7.** (a) View of the two-dimensional sheet constructed by 2,5-pydc$^{A}$ dianions bridging La$^{III}$ centers in **2**. (b) View of the tape of 2,5-pydc$^{B}$ dianions bridging La$^{III}$ atoms in **2**. (c) Perspective view of the three-dimensional framework of **2**.

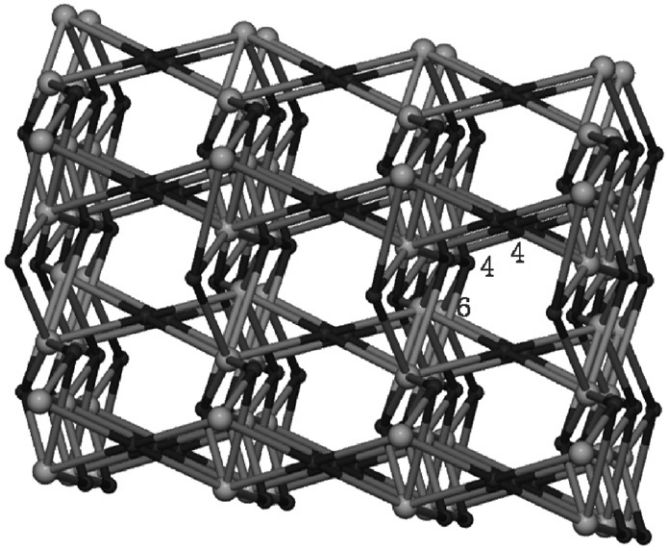


**Fig. 8.** Topological view of the (4,4,6)-connected net of **2** with $(4^28^4)(4^46^2)_2(4^96^6)_2$ circuit symbol.

decreases, a progressive depopulation of these levels occurs. Therefore, the nature of the coupling between the Yb$^{III}$ ions can not be unambiguously deduced only from the shape of the $\chi_mT$ vs $T$ curve. The continuous decrease of the $\chi_mT$ value for **1** may be due to the depopulation of the stark levels for a single Yb$^{III}$ ion and/or the antiferromagnetic inactions between Yb$^{III}$ ions within the $\mu$-O bridged chain.

### 2.6. TGA

TGA was carried out for crystalline samples of compounds **1**, **2** and **3** in the temperature range 25–800 °C (Fig. 12). For 1, the first loss of 3.78% in the range 100–220 °C corresponds to the loss of one coordinated and one lattice water molecule (calcd. 3.76%). The second weight loss above 350 °C corresponds to the decomposition of the coordination network. For **2**, the first weight loss of 4.38% is between 180 and 270 °C, which is attributed to the loss of water molecules (calcd. 4.44%). The second weight loss, 65.3%, occurred from 270–370 °C corresponds to the decomposition of the network. The third weight loss, 19.29%, occurred from 440 to 700 °C. For **3**, the first weight loss of 9.26% between 100 and 140 °C is attributed to the loss of water molecules (calcd. 10.30%). The second weight loss, 14.14%, occurred from 220 to 420 °C corresponds to the decomposition of the network. The third weight loss, 37.82%, occurred from 420 to 525 °C and the fourth weight loss of 8.55% occurred in the range of 525–695 °C.

## 3. Conclusions

In summary, we have synthesized three lanthanide–organic frameworks under hydrothermal conditions. Compound **1** represents an intricate three-dimensional network comprising intersecting moc-related (3,4)-connected and $CdSO_4$ net compound **2** exhibits a three-dimensional (4,4,6)-connected net with $(4^28^4)(4^46^2)_2(4^96^6)_2$ circuit symbol while compound **3** is a 2D layer based upon carboxylate-bridged La$^{III}$ chains. Such three nets not only enrich the database of topologies but also imply that coordination polymers represent powerful systems for investigation and defining new structures and topologies.

## 4. Experimental section

All chemicals are analytical grade and used without further purification. The hydrothermal reaction was performed in a 25 mL Teflon-lined stainless steel autoclave under autogenous pressure. Infrared spectra were recorded on a Magna 750 FT-IR spectrometer using KBr pellets. C, H and N microanalyses were measured with an elemental Vairo EL III analyzer. Powder X-ray diffraction (XRD) patterns of the samples were recorded by an X-ray diffractometer (RIGAKU-DMAX2500) with Cu$K\alpha$ radiation. Thermal analyses were performed using a thermal analyst 2100TA Instrument and a SDT 2960 simultaneous TGA-DTA instrument. The polycrystalline magnetic susceptibility data were collected on a Quantum Design PPMS model 6000 magnetometer in the temperature range from 2 to 300 K.

### 4.1. Synthesis of $[Yb_2(1,3\text{-pda})_3(H_2O)]_n \cdot nH_2O$ (**1**)

A mixture of $Yb(Ac)_3$ (0.035 g 0.1 mmol) and $H_2$1,3-pda (0.029 g, 0.15 mmol) in $H_2O$ (5 mL) was sealed in a 25 mL Teflon-lined bomb at 160 °C for 3 days, then slowly cooled to room temperature at a cooling rate of 5 °C h$^{-1}$. Colorless prismatic crystals were recovered by filtration, washed by distilled water,

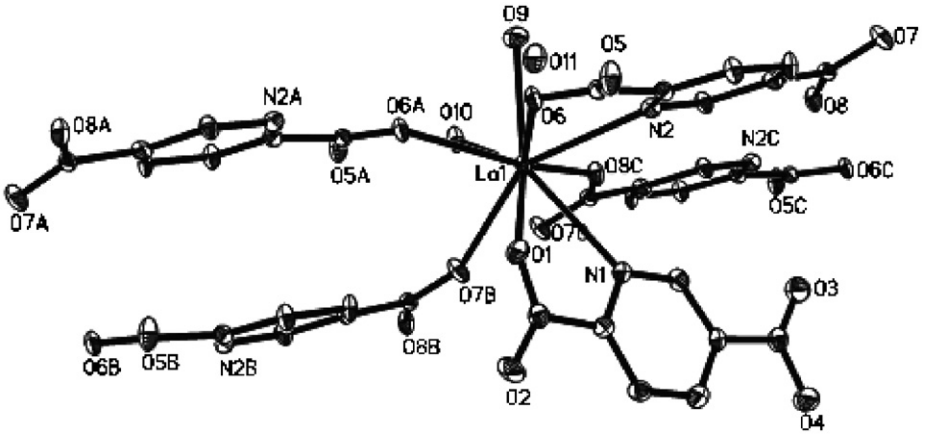


**Fig. 9.** The coordination environments of La atom in **3**. Symmetry codes: (A) 1−*x*, 1−*y*, 1−*z*; (B) 1+*x*, *y*, *z*; (C) −*x*, 1−*y*, 1−*z*; respectively.

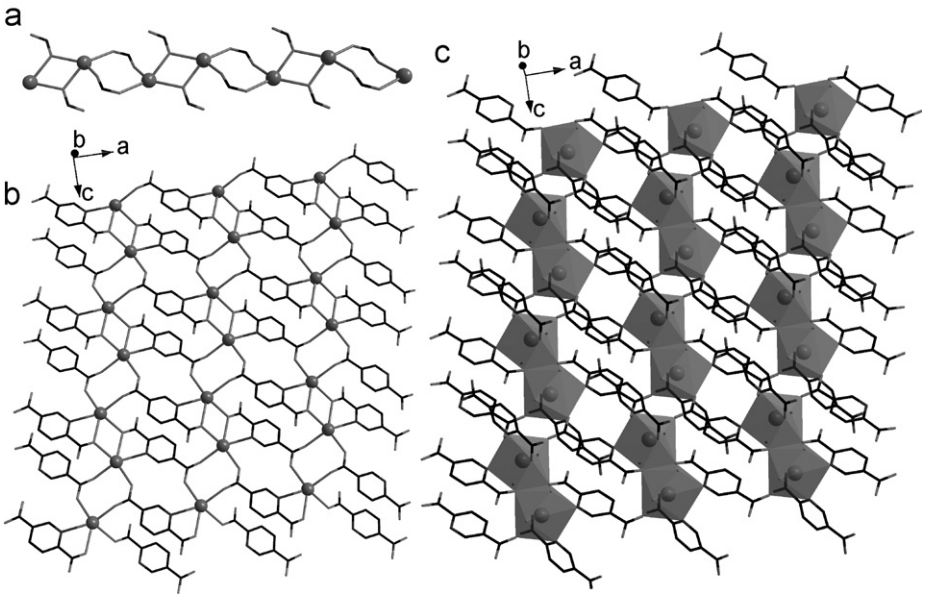


**Fig. 10.** (a) The carboxylate-bridged $La^{III}$ chain in **3**. (b) The layer formed by pyridine moities connected chains in **3**. (c) The whole layer structure of **3**.

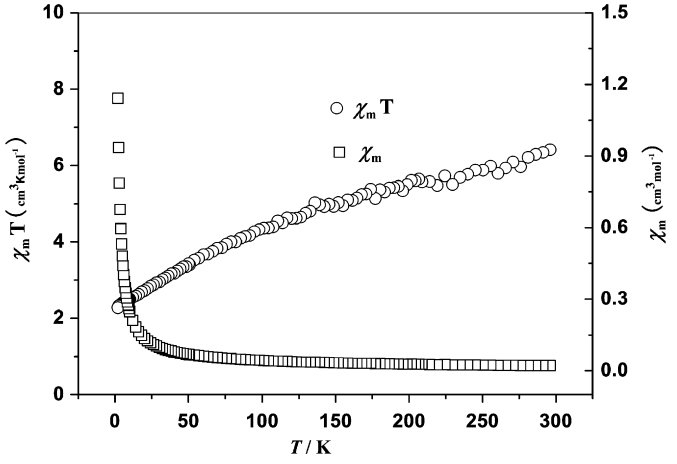


**Fig. 11.** Temperature-dependent $\chi_m T$ versus $T$ plot for **1**.

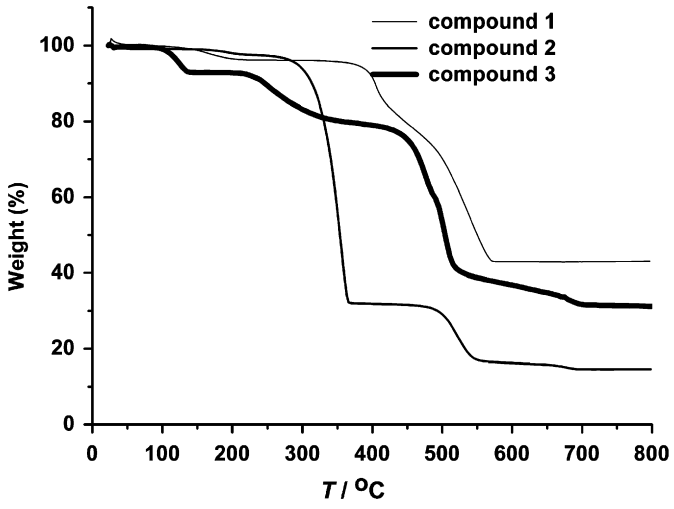


**Fig. 12.** TGA curves of **1**, **2** and **3**.

**Table 1**
Crystallographic data for **1**, **2** and **3**

| Compound | **1** | **2** | **3** |
|---|---|---|---|
| Formula | $C_{30}H_{28}O_{14}Yb_2$ | $C_{21}H_{13}La_2N_3O_{14}$ | $C_{14}H_{13}LaN_2O_{11}$ |
| Fw | 958.60 | 809.16 | 524.17 |
| Crystal size (mm) | 0.16 × 0.10 × 0.05 | 0.15 × 0.15 × 0.10 | 0.12 × 0.10 × 0.15 |
| Space group | $P2_1/c$ | $P2_1/c$ | $P2_1/c$ |
| $a$ (Å) | 12.071(2) | 6.5597(5) | 9.314(5) |
| $b$ (Å) | 17.678(3) | 18.0239(15) | 19.122(9) |
| $c$ (Å) | 14.737(2) | 9.4239(8) | 9.346(5) |
| $\beta$ (°) | 105.732(3) | 95.078(4) | 101.757(7) |
| $V$ (Å$^3$) | 3027.0(8) | 1109.83(16) | 1629.6(14) |
| Z | 4 | 2 | 4 |
| $\lambda$ (Mo$K\alpha$) (Å) | 0.71073 | 0.71073 | 0.71073 |
| $D_c$ (g cm$^{-3}$) | 2.103 | 2.421 | 2.137 |
| $\mu$ (mm$^{-1}$) | 6.213 | 3.886 | 2.692 |
| $T$ ($K$) | 293(2) | 293(2) | 293(2) |
| Reflns. collected | 22783 | 8427 | 12476 |
| Unique reflns. | 6864 | 2547 | 3223 |
| $R_{int}$ | 0.0271 | 0.0600 | 0.0567 |
| Parameters | 475 | 181 | 253 |
| $R_1$, w$R(I>2\sigma(I))$[a] | 0.0238, 0.0500 | 0.0334, 0.0801 | 0.0547, 0.1320 |
| $R_1$, w$R$(all data)[b] | 0.0269, 0.0516 | 0.0375, 0.0833 | 0.0648, 0.1412 |
| $W = 1/(\sigma^2(F_0^2)+(aP)^2+bP)$ | $a = 0.0193$, $b = 4.4422$ | $a = 0.0321$, $b = 0.8603$ | $a = 0.0529$, $b = 3.1138$ |
| Goodness-of-fit-on $F^2$ | 1.089 | 1.085 | 1.183 |
| $\Delta\rho_{min}$ and $\Delta\rho_{max}$ (e Å$^{-3}$) | −0.626, 0.872 | −1.103, 0.193 | −1.481, 1.743 |

[a] $R = \sum||F_0|-|F_c||/\sum|F_0|$.
[b] w$R = |\sum w(F_0-F_c)^2/\sum w(F_0^2)^2|^{1/2}$.

**Table 2**
Selected bond lengths (Å) and angles (°) for **1**

| Bond | | | |
|---|---|---|---|
| Yb1–O8H | 2.271 (2) | Yb1–O3D | 2.631 (3) |
| Yb1–O9B | 2.278 (2) | Yb2–O7G | 2.219 (2) |
| Yb1–O12 | 2.328 (2) | Yb2–O1 | 2.248 (2) |
| Yb1–O4D | 2.346 (3) | Yb2–O3E | 2.274 (3) |
| Yb1–O5 | 2.350 (2) | Yb2–O13 | 2.277 (3) |
| Yb1–O2 | 2.389 (2) | Yb2–O11 | 2.328 (3) |
| Yb1–O6 | 2.427 (2) | Yb2–O10 | 2.358 (3) |
| Yb1–O1 | 2.505 (2) | Yb2–O9 | 2.407 (2) |
| **Angle** | | | |
| O8H–Yb1–OB | 77.58 (9) | O5–Yb1–O3D | 128.18 (9) |
| O8H–Yb1–O12 | 76.95 (10) | O2–Yb1–O3D | 143.06 (8) |
| O9B–Yb1–O12 | 142.95 (9) | O6–Yb1–O3D | 110.32 (8) |
| O8H–Yb1–O4D | 126.38 (10) | O1–Yb1–O3D | 143.48 (8) |
| O9B–Yb1–O4D | 93.57 (10) | O5–Yb1–O3D | 128.18 (9) |
| O12–Yb1–O4D | 80.53 (11) | O7G–Yb2–O1 | 86.36 (9) |
| O8H–Yb1–O5 | 145.44 (8) | O7G–Yb2–O3E | 86.76 (9) |
| O9B–Yb1–O5 | 130.95 (8) | O1–Yb2–O3E | 158.76 (9) |
| O12–Yb1–O5 | 83.60 (9) | O7G–Yb2–O13 | 87.15 (10) |
| O4D–Yb1–O5 | 76.94 (9) | O1–Yb2–O13 | 80.55 (9) |
| O8H–Yb1–O2 | 78.05 (10) | O3E–Yb2–O13 | 79.06 (10) |
| O9B–Yb1–O2 | 82.26 (9) | O7G–Yb2–O11 | 157.60 (10) |
| O12–Yb1–O2 | 117.77 (9) | O1–Yb2–O11 | 111.38 (10) |
| O4D–Yb1–O2 | 153.90 (10) | O3E–Yb2–O11 | 80.95 (12) |
| O5–Yb1–O2 | 86.37 (9) | O13–Yb2–O11 | 108.58 (14) |
| O8H–Yb1–O6 | 146.53 (9) | O7G–Yb2–O10 | 89.85 (12) |
| O9B–Yb1–O6 | 76.87 (8) | O1–Yb2–O10 | 76.89 (10) |
| O12–Yb1–O6 | 135.23 (9) | O3E–Yb2–O10 | 123.17 (10) |
| O4D–Yb1–O6 | 76.55 (10) | O13–Yb2–O10 | 157.38 (10) |
| O5–Yb1–O6 | 54.09 (8) | O11–Yb2–O10 | 81.45 (16) |
| O2–Yb1–O6 | 77.42 (9) | O7G–Yb2–O9 | 79.23 (9) |
| O8H–Yb1–O1 | 76.49 (8) | O1–Yb2–O9 | 128.41 (9) |
| O9B–Yb1–O1 | 131.54 (9) | O3E–Yb2–O9 | 69.64 (10) |
| O12–Yb1–O1 | 66.36 (9) | O13–Yb2–O9 | 146.34 (8) |
| O4D–Yb1–O1 | 134.61 (9) | O11–Yb2–O9 | 78.96 (11) |
| O5–Yb1–O1 | 69.56 (8) | O10–Yb2–O9 | 54.07 (9) |
| O2–Yb1–O1 | 52.70 (8) | O7G–Yb2–O12 | 150.11 (8) |
| O6–Yb1–O1 | 105.49 (8) | O1–Yb2–O12 | 65.99 (8) |
| O8H–Yb1–O3D | 77.68 (9) | O3E–Yb2–O12 | 114.80 (9) |
| O9B–Yb1–O3D | 65.59 (9) | O13–Yb2–O12 | 77.66 (9) |
| O12–Yb1–O3D | 82.97 (9) | O11–Yb2–O12 | 51.84 (9) |
| O4D–Yb1–O3D | 51.54 (8) | O10–Yb2–O12 | 94.42 (11) |

Symmetry codes: (B) $x$, 1/2−$y$, 1/2+$z$; (D) −1+$x$, $y$, $z$; (E) −1+$x$, 1/2−$y$, −1/2+$z$; (D) 2−$x$, −$y$, −$z$; (H) 2−$x$, 1/2+$y$, 1/2−$z$.

and air-dried (yield: 82% based on $Yb(Ac)_3$). The positions of the diffraction peaks of the experimental and simulated XRD patterns correspond well, thus indicating phase purity of the as-synthesized samples (Fig. S1). Elemental analysis calcd. (%) for $C_{30}H_{28}Yb_2O_{14}$ (**1**): C 37.55, H 2.92. Found: C 37.51, H 2.86. IR data (KBr cm$^{-1}$): 3416(b), 2365(w), 1641(s), 1618(s), 1400(s) 1392(s), 1264(w), 1143(w), 956(m), 734(m), 617(w).

### 4.2. Synthesis of $[La_2(2,5\text{-}pydc)_3(H_2O)_2]_n$ (**2**)

A mixture of $La_2O_3$ (0.033 g, 0.1 mmol) and $H_2$pydc (0.024 g, 0.15 mmol) in $H_2O$ (10 mL) was adjusted to pH = 4 with HCl and sealed in a 25 mL Teflon-lined bomb at 160 °C for 3 days, then slowly cooled to room temperature at a cooling rate of 5 °C h$^{-1}$. Colorless prismatic crystals were recovered by filtration, washed by distilled water, and air-dried (yield: 66% based on $H_2$pydc). The positions of the diffraction peaks of the experimental and simulated XRD patterns correspond well, thus indicating phase purity of the as-synthesized samples (Fig. S2). Elemental analysis calcd. (%) for $C_{21}H_{13}La_2N_3O_{14}$ (**2**): C 31.43, H 1.61. N 5.19. Found: C 31.36, H 1.58. 5.16 IR data (KBr cm$^{-1}$): 3466(b), 1633(s), 1614(s), 1404(s), 1283(w), 1108(w), 835(w), 761(w), 606(w).

### 4.3. Synthesis of $[La(2,5\text{-}pydc)(2,5\text{-}Hpydc)(H_2O)_2]_n \cdot nH_2O$ (**3**)

A mixture of $La(NO_3)_3 \cdot 6H_2O$ (0.087 g, 0.2 mmol) and $H_2$pydc (0.064 g, 0.4 mmol) in $H_2O$ (10 mL) was sealed in a 25 mL Teflon-lined bomb at 160 °C for 3 days, then slowly cooled to room temperature at a cooling rate of 5 °C h$^{-1}$. Colorless prismatic crystals were recovered by filtration, washed by distilled water, and air-dried (yield: 71% based on $H_2$pydc). The positions of the diffraction peaks of the experimental and simulated XRD patterns correspond well, thus indicating phase purity of the as-synthesized samples (Fig. S3). Elemental analysis calcd. (%) for $C_{14}H_{13}LaN_2O_{11}$ (**3**): C 32.05, H 2.48. N 5.34. Found: C 31.99, H 2.45. 5.31 IR data (KBr cm$^{-1}$): 3462(b), 16383(s), 1617(s), 1400(s), 1281(w), 1110(w), 838(w), 762(w), 608(w).

### 4.4. X-ray crystallography

Data collections were performed at 293(2) K on a Mercury CCD diffractometer with graphite monochromated Mo$K\alpha$ radiation ($\lambda = 0.71073$ Å). The structures were solved by direct methods and all calculations were performed using the SHELXL package [35]. The structure were refined by full matrix least squares with anisotropic displacement parameters for non-hydrogen atoms. For **1**, no attempt was made to locate the H atoms of water molecules and the other H atoms were generated geometrically and treated as riding. For **2** and **3**, all hydrogen atoms belonging to the water molecules and carboxyl groups were found in the electron density map and refined isotropically, the other H atoms were generated geometrically and treated as riding. The crystallographic data are summarized in Table 1 and selected bond lengths and bond angles

**Table 3**
Selected bond lengths (Å) and angles (°) for **2**

| Bond | | | |
|---|---|---|---|
| La1–O5B | 2.467 (3) | La1–O7 | 2.627 (3) |
| La1–O6C | 2.475 (3) | La1–O2A | 2.644 (3) |
| La1–O3 | 2.475 (3) | La1–O1A | 2.699 (3) |
| La1–O4D | 2.514 (3) | La1–N1 | 2.746 (3) |
| La1–O1 | 2.547 (3) | | |
| **Angle** | | | |
| O5B–La1–O6C | 140.84 (10) | O1–La1–O2A | 90.79 (9) |
| O5B–La1–O3 | 131.99 (10) | O7–La1–O2A | 92.27 (10) |
| O6C–La1–O3 | 85.45 (10) | O5B–La1–O1A | 98.51 (9) |
| O5B–La1–O4D | 76.02 (10) | O6C–La1–O1A | 78.62 (9) |
| O6C–La1–O4D | 79.57 (9) | O3–La1–O1A | 74.67 (10) |
| O3–La1–O4D | 140.36 (10) | O4D–La1–O1A | 136.04 (9) |
| O5B–La1–O1 | 71.06 (9) | O1–La1–O1A | 138.42 (9) |
| O6C–La1–O1 | 134.70 (9) | O7–La1–O1A | 68.45 (9) |
| O3–La1–O1 | 83.17 (10) | O2A–La1–O1A | 49.08 (8) |
| O4D–La1–O1 | 81.89 (10) | O5B–La1–N1 | 124.27 (10) |
| O5B–La1–O7 | 66.74 (10) | O6C–La1–N1 | 74.36 (9) |
| O6C–La1–O7 | 76.25 (10) | O3–La1–N1 | 69.13 (10) |
| O3–La1–O7 | 141.27 (10) | O4D–La1–N1 | 71.53 (9) |
| O4D–La1–O7 | 69.51 (9) | O1–La1–N1 | 60.60 (9) |
| O1–La1–O7 | 133.29 (9) | O7–La1–N1 | 134.47 (9) |
| O5B–La1–O2A | 69.18 (10) | O2A–La1–N1 | 133.22 (9) |
| O6C–La1–O2A | 126.33 (9) | O1A–La1–N1 | 135.94 (9) |
| O3–La1–O2A | 71.50 (10) | O1–La1–O2$^{A}$ | 90.79 (9) |

Symmetry codes: (A) $x$, 1/2−$y$, −1/2+$z$; (B) 1−$x$, −1/2+$y$, 3/2−$z$; (C) 1−$x$, 1−$y$, 1−$z$; (D) −1+$x$, $y$, $z$.

**Table 4**
Selected bond lengths (Å) and angles (°) for **3**

| Bond | | | |
|---|---|---|---|
| La1–O7B | La1–O7B | La1–O6A | 2.603 (4) |
| La1–O8C | La1–O8C | La1–O6 | 2.639 (5) |
| La1–O9 | La1–O9 | La1–N2 | 2.732 (5) |
| La1–O1 | La1–O1 | La1–N1 | 2.796 (5) |
| La1–O10 | La1–O10 | Yb2–O13 | 2.277 (3) |
| **Angle** | | | |
| O7B–La1–O8C | 91.55 (16) | O1–La1–O6 | 66.29 (15) |
| O7B–La1–O9 | 137.86 (17) | O10–La1–O6 | 131.96 (15) |
| O8C–La1–O9 | 88.47 (15) | O6A–La1–O6 | 65.93 (16) |
| O7B–La1–O1 | 70.51 (16) | O7B–La1–N2 | 147.27 (16) |
| O8C–La1–O1 | 128.24 (15) | O8C–La1–N2 | 74.90 (15) |
| O9–La1–O1 | 137.19 (16) | O9–La1–N2 | 72.57 (16) |
| O7B–La1–O10 | 71.89 (16) | O1–La1–N2 | 94.41 (15) |
| O8C–La1–O10 | 69.57 (15) | O10–La1–N2 | 127.17 (15) |
| O9–La1–O10 | 68.73 (18) | O6A–La1–N2 | 124.48 (15) |
| O1–La1–O10 | 138.35 (15) | O6–La1–N2 | 61.32 (14) |
| O7B–La1–O6A | 82.24 (15) | O7B–La1–N1 | 76.19 (16) |
| O8C–La1–O6A | 147.96 (15) | O8C–La1–N1 | 69.42 (15) |
| O9–La1–O6A | 75.99 (15) | O9–La1–N1 | 141.28 (16) |
| O1–La1–O6A | 79.18 (14) | O1–La1–N1 | 59.35 (16) |
| O10–La1–O6A | 78.65 (15) | O10–La1–N1 | 126.35 (16) |
| O7B–La1–O6 | 129.82 (14) | O6A–La1–N1 | 137.57 (15) |
| O8C–La1–O6 | 135.49 (14) | O6–La1–N1 | 101.59 (15) |
| O9–La1–O6 | 71.86 (16) | N2–La1–N1 | 71.18 (16) |

Symmetry codes: (A) 1−$x$, 1−$y$, 1−$z$; (B) 1+$x$, $y$, $z$; (C) −$x$, 1−$y$, 1−$z$.

of **1**, **2** and **3** are listed in Tables 2–4. CCDC-659032 (**1**), 659033 (**2**) and 679629 (**3**) contain the supplementary crystallographic data for this paper.

## Acknowledgments

This work was supported by the grants of the National Natural Science Foundation of China and the Natural Science Foundation of Fujian Province and The Young Scientist Funds of Fujian Province (Nos. 2006F3130 and 2006F3138). We thank the referees for their excellent suggestions and valuable insight into the topologies.

## Appendix A. Supplementary data

Supplementary data associated with this article can be found in the online version at doi:10.1016/j.jssc.2008.09.021.

## References

[1] A.J. Blake, N.R. Champness, P. Hubberstey, W.S. Li, M.A. Withersby, M. Schröder, Coord. Chem. Rev. 183 (1999) 117.
[2] M.L. Tong, X.M. Chen, S.R. Batten, J.Am. Chem. Soc. 125 (2003) 16170.
[3] M. Eddaoudi, J. Kim, M. O'Kefffe, O.M. Yaghi, J. Am. Chem. Soc. 124 (2002) 367.
[4] B. Rather, B. Moulton, R.D.B. Walsh, M.J. Zaworotko, Chem. Commun. (2002) 694.
[5] L. Carlucci, N. Cozzi, G. Ciani, M. Moret, D.M. Proserpio, S. Rizzato, Chem. Commun. (2002) 1354.
[6] X.H. Huang, T.L. Sheng, S.C. Xiang, R.B. Fu, S.M. Hu, Y.M. Li, X.T. Wu, Inorg. Chem. 46 (2007) 497.
[7] M.C. Hong, Cryst. Growth Des. 7 (2007) 10.
[8] M.J. Zaworotko, Cryst. Growth Des. 7 (2007) 4.
[9] X. Li, R. Cao, D.F. Sun, W.H. Bi, D.Q. Yuan, Eur. J. Inorg. Chem. (2004) 2228.
[10] C.Z. Xie, Z.F. Zhang, B.F. Zhang, X.Q. Wang, R.J. Wang, G.Q. Shen, D.Z. Shen, B. Ding, Eur. J. Inorg. Chem. (2006) 1337.
[11] A.F. Wells, Further Studies of Three-Dimensional Nets, American Crystallographic Association (distributed by Polycrystal Book Service), New York (Pittsburgh, PA), 1979.
[12] A.F. Wells, Three-Dimensional Nets and Polyhedra, Wiley, New York, 1977.
[13] O.D. Friedrichs, M. O'Kefffe, O.M. Yaghi, Acta Crystallogr.: Sect. A 59 (2003) 22.
[14] M. O'Kefffe, M. Eddaoudi, H. Li, T. Reineke, O.M. Yaghi, J. Solid State Chem. 157 (2000) 3.
[15] R.J. Robson, ., J.Chem. Soc., Dalton Trans (2000) 3735.
[16] B. Moulton, H. Abourahma, M.W. Brander, J. Lu, G.J. McManus, M.J. Zaworotko, Chem. Commun. (2003) 1342.
[17] C. Qin, X.L. Wang, E.B. Wang, Su, Z.M. Inorg. Chem. 44 (2005) 7122.
[18] D.-L. Long, A.J. Blake, N.R. Champness, C. Wilson, M. Schröder, J. Am. Chem. Soc. 123 (2003) 3401.
[19] D.-L. Long, A.J. Blake, N.R. Champness, C. Wilson, M. Schröder, Chem. Commun. (2000) 1369.
[20] R.J. Hill, D.-L. Long, M.S. Turvey, A.J. Blake, N.R. Champness, P. Hubberstey, C. Wilson, M. Schröder, Chem. Commun. (2004) 1792.
[21] M. Oh, G.B. Carpenter, D.A. Sweigart, Angew. Chem. Int. Ed. 42 (2003) 2026.
[22] R. Natarajan, G. Savitha, P. Dominiak, K. Wozniak, J.H. Moorthy, Angew. Chem. Int. Ed. 44 (2005) 2115.
[23] D.-F. Sun, D.J. Collins, Y.-X. Ke, J.-L. Zuo, H.-C. Zhou, Chem. Eur. J. 12 (2005) 1792.
[24] Y.-Q. Lan, X.-L. Wang, L.-S. Li, Z.-M. Su, K.-Z. Shao, E.-B. Wang, Chem. Commun. (2007) 4863.
[25] M.A.M. Abu-youssef, V. Langer, L. Öhrström, Chem. Commun. (2006) 1082.
[26] D.N. Dybtsev, H. Chun, K. Kim, Chem. Commun. (2004) 15942.
[27] D.T. Nguyen, E. Chew, Q.-C. Zhang, A. Choi, X.-H. Bu, Inorg. Chem. 45 (2006) 10722.
[28] N.W. Ockwig, O. Delgado-Friederichs, M. O'Keeffee, O.M. Yaghi, Acc. Chem. Res. 38 (2005) 176.
[29] Y.G. Huang, B.L. Wu, D.Q. Yuan, Y.Q. Xu, F.L. Jiang, M.C. Hong, Inorg. Chem. 46 (2007) 1171.
[30] See website: 〈http://rcsr.anu.edu.au/〉.
[31] Y.F. Zhou, R.H. Wang, B.L. Wu, R. Cao, M.C. Hong, J. Mol. Struct. 697 (2004) 73.
[32] A.D. Burrows, A.S. Donovan, R.W. Harrington, M.F. Mahon, Eur. J. Inorg. Chem. (2004) 4686.
[33] J.-C.G. Bunzli, G.R. Chopin, Lanthanide Probes in Life Chemical and Earth Sciences, Elsevier, Amsterdam, 1989.
[34] H.L. Gao, L. Yi, X.Q. Zhao, P. Cheng, D.Z. Liao, S.P. Yan, Inorg. Chem. 45 (2006) 5980.
[35] G.M. Sheldrick, SHELXTL-97, Program for the Solution of Crystal Structures, University of Göttingen, Germany, 1997.